STRUCTURAL, MORPHOLOGICAL AND OPTICAL PROPERTIES OF ANNEALED Cu_2ZnSnS_4 THIN FILMS USING THE FIRST DERIVATIVE OF TGA CURVE FOR SOLAR CELL APPLICATIONS

A. ALMOHAMMEDI[a], A. ASHOUR[a,b], E. R. SHAABAN[c,]
[a]*Physics Department, Faculty of Science, Islamic University, P. O. Box 170, Al Madinah, Saudi Arabia*
[b]*Physics Department, Faculty of Science, Minia University, El Minia, Egypt*
[c]*Physics Department, Faculty of Science, Al–Azhar University, Assuit, 71542, Egypt*

Structural, morphological and optical properties of Cu_2ZnSnS_4 (CZTS) thin films as a function of annealing temperature in terms of the first derivative of TGA curve on glass substrates by thermal evaporation method. The thicknesses of the films were about 900 nm. Their structure and composition are studied by X-ray diffraction, scanning electron microscopy, Raman spectrum and optical absorbance measurements. All the films exhibited kesterite structure with preferential orientation along the (112) direction. The variations of the Microstructural parameters, such as crystallite size and lattice strain with annealing temperature were studied. The results show the crystallite sizes increase but the lattice strains decrease with increasing annealing temperature. SEM of the CZTS thin film annealed at 500 °C exhibited large agglomeration of crystallites size. The energy gap was calculated using the first derivative of absorbance spectra that decreases with increasing annealing temperature. The results confirm that the CZTS thin film annealed at 500 °C exhibited large agglomeration of grains and ideal band gap (E_g = 1.28 eV) for absorbing layer of solar cell.

(Received September 1, 2019; Accepted January 10, 2020)

Keywords: Cu_2ZnSnS_4; thin film; TGA**;** SEM**;** Raman spectrum; Energy gap

1. Introduction

There is an increased interest in renewable energy sources in terms of grid parity proximity. In particular, photovoltaic (PV) systems exhibit great potential in this area because they use solar energy that is abundantly available globally [1]. Materials used in photovoltaic devices should be cheap, abundantly available in nature, and environmentally friendly. In this respect, Cu_2ZnSnS_4 (CZTS) thin films are appropriate for use in photovoltaic devices [2]. Further, CZTS thin films exhibit a Direct band gap of 1.4-1.5 eV, which enables of PV solar cell to suitable convert solar energy into electrical energy with a large absorption coefficient above 10^4 cm^{-1}, low thermal conductivity etc [3]. It is derived from the CIGS structure by the isoelectronic substitution of two In (or one In and one Ga) atoms by one Zn and one Sn atom. As a consequence, CZTS has some similar properties as CIGS. The availability of Cu, Zn, Sn and S in the earth's crust are ~ 50, 75, 2.2 and 260 ppm respectively and the availability of In is only ~0.049 ppm [4], so that all the constituents of CZTS are abundant in the earth's crust. Intrinsic point defects in CZTS make its conductivity p-type. Crystal structure of CZTS can allow some deviation from stoichiometry [5] making its deposition process easier. Moreover, grain boundaries in CZTS thin films are favorable to enhance the minority carrier collection [6]. Theoretical calculations have shown that conversion efficiency as high as 32.2 % [7] is possible for CZTS thin film solar cells with a CZTS layer of few micrometers. *Wadia et al.* [8] calculated the minimum cost of raw materials for the existing PV technologies and the emerging PV technologies and found that the cost of raw material for CZTS PV technology is much lower than that of the existing thin film PV technologies. Various methods have been applied for CZTS thin film fabrication which includes solution methods [9-11], sol-gel [12, 13], electroplating [14, 15], co-evaporation [16], pulsed laser deposition [17, 18], evaporation [19, 20] etc. In this study, CZTS was synthesized using simple chemical reaction method in order to prepare a solid bulk compound CZTS target material for thermal evaporation

* Corresponding author: arda@iu.edu.sa

deposition. CZTS thin films were prepared by using vacuum thermal evaporation technique. The influences of annealing temperature (in terms the derivative of TGA curve) on the structural, morphological and optical properties of CZTS thin films were studied.

2. Experimental details

In the present work, the synthesis of CZT precursors by using $Cu(NO_3)_2$, $Zn(CH_3COO)_2$ and $SnCl_2$ in a mixture of 2, 1 and 1 mol/L were dissolved into the deionized water containing citric acid (molar ratio for ion of metal to citric acid is 1:3) and stirred in the flask for 10 min to obtain transparent solution. Citric acid was used as the complexing agent. For preparing CZTS the temperature of the solution is 5 ^{o}C/min. when the temperature reaches 200 ^{o}C, 4 mL sulfur-oleylamine solution is added into the flask and reacted for 30 min. after the reaction is completed, CZTS nanoparticles are separated using centrifuge. The final solution is dried in a furnace in low vacuum for obtaining the powder sample. The obtained powder was then pressed into a disk–shape pellet. Such pellets were used as the starting materials from which the thin film will be prepared. The thermogravimetric analysis of the Cu_2ZnSnS_4 nanoparticle is obtained using TGA instruments (Shimadzu 50 with an accuracy of ±0.1 K). Twenty mg powdered sample, crimped into aluminum pans was scanned at heating rate (β = 5 ^{o}C/min). Cu_2ZnSnS_4 thin films were prepared by thermal evaporation technique via a coating unit (Denton Vacuum DV 502 A) under high vacuum conditions (10^{-7} mbr). The substrates utilized for deposition were carefully cleaned using ultrasonic hot bath distilled water and pure alcohol before the evaporation process started. The thickness of the as-deposited films studied is mostly about 100 nm in order to avoid the effect of film thickness. During the deposition process, the substrates were kept at temperature equal 150 ^{o}C and the deposition rate was adjusted at 20 Å/sec. The substrates were rotated at slow speed 5 Rev/min to obtain a homogenous and smooth film. During evaporation process, the thickness of the produced films was monitored using FTM6 thickness monitor**.**

X-ray powder diffraction (XRD) Philips diffractometry (1710), with Cu-$K_{\alpha 1}$ radiation (λ = 1.54056 Å) have been used to examine the structure of the as prepared and annealed Cu_2ZnSnS_4 films. The data collection was performed by step scan mode, in a 2θ range between 5° and 80° with step-size of 0.02° and step time of 0.6 seconds. Pure Silicon~ Si 99.9999% was used as an internal standard. The chemical composition of the Cu_2ZnSnS_4 films were assessed by using energy dispersive X-ray spectrometer unit (EDXS) interfaced with a scanning electron microscope (SEM, JOEL XL) operating an accelerating voltage of 30 kV, used for the morphology studies. The relative error of elements determination does not exceed 3 %, during the analysis. The absorbance spectra for as-deposited and annealed films were obtained by a double-beam computer-controlled spectrophotometer (UV-2101, Shimadzu) at normal light incidence in the range of wavelength from 400 to 1500 nm.

3. Results and discussion

Thermogravimetric analysis (TGA) analysis was performed to study the change of phases by heating the CZTS nanoparticle with heating rate 10 ^{o}C/min extended from room temperature to 600 ^{o}C. The simultaneous TGA graph and its differentiation are shown in Fig. 1. The differentiation of TGA curve is very important for identifying the peaks with high precision. The TGA curve has two main slopes. The first slope from RT to 100 ^{o}C is affected by the evaporation of strongly volatile of organics and the second slope from 100 to 185 ^{o}C is affected by the phenomenon of the boiling of the boiling of the hexanethiol solvent. The differentiation curve has three main phases at 35 to 100 ^{o}C, 100 to 185 ^{o}C and the third phase around 500 ^{o}C that represent the maximum crystallization peak. So, the annealing temperatures were chosen at 400 ^{o}C, 450 ^{o}C, 475 ^{o}C and 500 ^{o}C (Max. crystallization temperature).

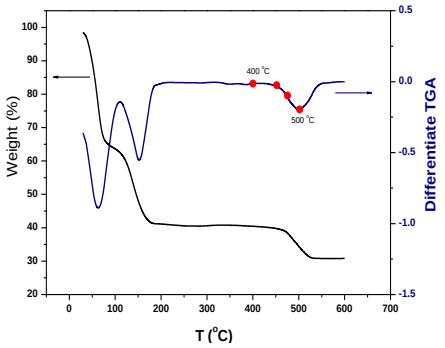

Fig. 1. The simultaneous TGA and its differentiation curves for Cu_2ZnSnS_4 nanoparticle precursor.

X-ray diffraction (XRD) patterns for as-grown and annealed CZTS thin films are shown in Fig. 2. The as-grown material shows three broad peaks, which can be correlated with the three main peaks in the powder diffraction file of bulk kesterite CZTS (JCPDS 26-0575, a = 5.435 Å, c = 10.869 Å), (112), (220) and (312) at 2θ = 28.53°, 47.33° and 56.18°, as the annealing temperature increases the intensity of the peaks increase, i.e. the crystallinity of CZTS thin films increase with annealing temperature. The optimal crystallinity was at 500 °C according to the differentiation of TGA curve.

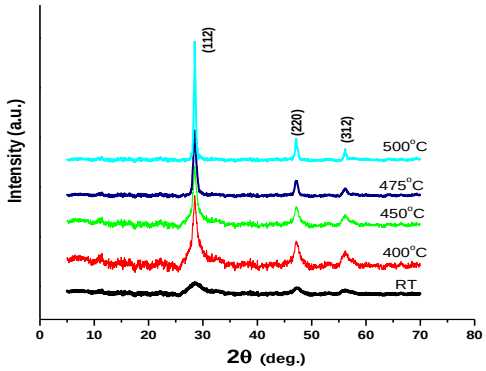

Fig. 2. XRD pattern of as-deposited and annealing temperature of CZTS thin film.

Both crystallize size (*D*) and lattice strain *(e)* were determined using the Scherrer and Wilson equations [21-33]:

$$D = \frac{0.9\lambda}{\beta \cos\theta} \tag{1}$$

$$e = \frac{\beta}{4\tan\theta} \tag{2}$$

where β is the structural broadening that equals the difference in integral X-ray peak profile width which between the sample and the standard (silicon) and is given as: $\beta = \sqrt{\beta_{obs}^2 - \beta_{std}^2}$.

It is observed that the average crystallite size increases (from 12 nm to 75 nm) but the lattice strain decreases (from 7.2 x10^{-3} to 1.8 x10^{-3}) when the annealing temperature increases.

The Raman spectrum of the CZTS thin films also confirms the CZTS structure as shown in Fig. 3. The major scattering peaks of the CZTS thin films appear at 290 cm^{-1}, 337 cm^{-1} and 370 cm^{-1} that representative of the kesterite CZTS structure [24, 25]. Another peak positioned at about 474 cm^{-1}, which can be assigned to the $Cu_{2-x}S$ phase in terms of the Raman detection but was difficult to determine using XRD or disappear with the amorphous hump of glass substrate. As the annealing temperature increase the scattering peaks are shifted towards to the lower Raman shift. The results indicated that there were no cubic ZnS, tetragonal Cu_2SnS_3, and cubic Cu_2SnS_3. High quality CZTS nanocrystals could be obtained by the above mentioned synthesized method.

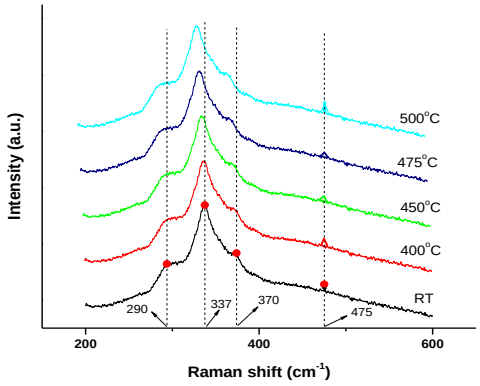

Fig. 3. Raman spectrum analysis of CZTS thin film according to change of annealing temperature.

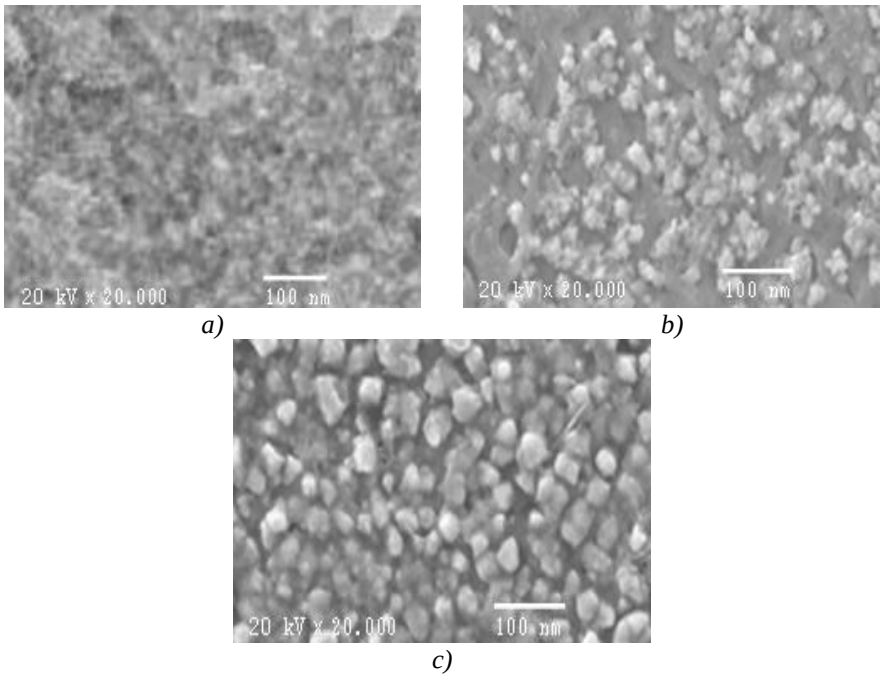

Fig. 4. SEM images of CZTS thin films at temperatures a)As deposited, (b) 400 °C c)500 °C

Fig. 4 shows scanning electron micrograph images of the CZTS thin films of the as deposited and annealed temperature at 400 °C and 500 °C. All samples are covered with grains with different sizes. For the CZTS thin film at 400 °C, the surface shows a fair crystalline quality with few voids and the average grain size was about 30 nm. Larger agglomeration of grains in the CZTS thin film at 500 °C than those at 400 and the average grain size was 50 nm which is beneficial in

photovoltaic application. It is concluded that a high annealing temperature can improve the crystallinity and grain sizes.

The double beam spectrophotometer was adopted to measure the absorbance in wavelength range extended from 400 to 1500 nm for the as deposited and annealed CZTS thin films (see Fig. 5). When photons are incident on CZTS films, they will be absorbed only when the minimum energy of photons is enough to excite an electron from the valence band to conduction band or when the photon energy equal to the energy gap of the material. This figure shows that the absorbance shifted towards higher wavelength with increasing the annealing temperature. In order to extract the energy gap, E_g^{opt} value, the first derivative of absorbance with respect to wavelength was considered. Fig. 6 shows the differentiation of absorbance with respect to wavelength as a function of wavelength for the as deposited and annealed samples. Fig. 6 also shows that the position of the peaks shifted to the higher wavelength. The all peaks that appear in this Figure are due to the electronic transitions from fundamental band edge. The position of the peak has been used to estimate the band gap energy E_g^{opt} [26-28]. The estimated optical band gap found to be decreased from 2.14 to 1.28 eV with increasing the annealing temperature of CZTS thin film. The decreasing in optical band gap may be attributed to the increasing of crystallize size with increasing the annealing temperature. The crystallize size is made up a large number of atoms, so, the number of overlapping of orbitals or energy level increases and the width of the band gets wider. This will cause a decrease in energy gap between the valance band and the conduction band.

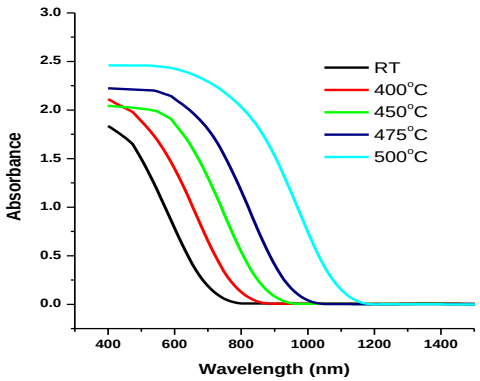

Fig. 5. Typical absorbance spectra of as-deposited and annealing temperature of CZTS thin film.

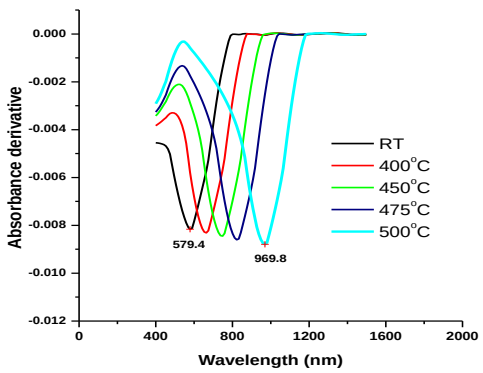

Fig. 6. Absorbance derivative as a function of wavelength for as-deposited and annealing temperature of CZTS thin film.

4. Conclusions

In this study, CZTS was synthesized using simple chemical reaction method. CZTS thin films were prepared by using vacuum thermal evaporation technique. The influences of annealing temperature (in terms the derivative of TGA curve) on the structural, morphological and optical properties of CZTS thin films were studied. XRD analysis shows that all the films exhibited kesterite structure with preferential orientation along the (112) direction. The average crystallite size increases (from 12 nm to 75 nm) but the lattice strain decreases (from 7.2 $x10^{-3}$ to 1.8 $x10^{-3}$) when the annealing temperature increases.

The Raman spectrum of the CZTS thin films also confirm the CZTS structure with a small trace of $Cu_{2-x}S$ phase that was difficult to determine using XRD or disappear with the amorphous hump of glass substrate. SEM of the CZTS thin film annealed at 500 °C exhibited large agglomeration of crystallites size. It is concluded that a high annealing temperature can improve the crystallinity and grain sizes. The energy gap, E_g^{opt} value was estimated in terms of peaks of the first derivative of absorbance with respect to wavelength. All the position of the peaks shifted to the higher wavelength, i.e. E_g^{opt} decreases from decreases from 2.14 to 1.28 eV with increasing the annealing temperature of CZTS thin film. The results confirm that the CZTS thin film annealed at 500 °C exhibited large agglomeration of grains and ideal band gap (E_g = 1.28 eV) for absorbing layer of solar cell.

Acknowledgments

The authors are grateful to Assiut University and Al-Azhar University (Assiut branch) for supporting with the experimental measurements. In addition, the authors thank the Deanship of Scientific Research at Islamic University, Al Madinah, Saudi Arabia for funding this research via project number: (9/40 - 1440-1441 AH).

References

[1] C. Breyer, A. Gerlach, Progress in photovoltaic, 21 (2013).
[2] V. Tunuguntle, W. Chen, P. Shih, J. Mat. C. **A3**, 15324 (2015).
[3] T. Tanaka, T. Nagatomo, D. Kawasaki, J. Phys. Chem. Solids **66**, 1978 (2005).
[4] M. I. Hossain.. Chalcogen Lett. **9**, 231 (2012).
[5] L. Choubrac, A. Lafond, C. Guillot-Deudon, Y. Moëlo, S. Jobic. Inorg Chem **51**, 3346 (2012).
[6] J. B. Li, V. Chawla, B. M. Clemens. Adv Mater. **24**, 720 (2012).
[7] W. Shockley, HJ Queisser. Jpn. J. Appl. Phys. **32**, 510 (1961).
[8] C. Wadia, AP Alivisatos, D Kammen. Environ Sci Technol. **43**, 2072 (2009).
[9] O. Zaberca, A. Gillorin, B. Durand, J. Y. Chane-Ching. J. Mater. Chem. **21**, 6483 (2011).
[10] N. M. Shinde, C. D. Lokhande, J. H. Kim, Moon. J. Photochem. Photobio. A **235**, 14 (2012).
[11] T. Rath, W. Haas, A. Pein. Sol Energy Mater.: Sol. Cells **101**, 87 (2012).
[12] K. Tanaka, N. Moritake, H. Uchiki. Sol. Energy Mater.: Sol. Cells **91**, 1199 (2007).
[13] M. Y. Yeh, C. C. Lee, D. S. Wuu, J. Sol-Gel Sci Technol. **52**, 65 (2009).
[14] C. P. Chan, H. Lam, C. Surya, Sol. Energy Mater. Sol Cells **94**, 207 (2010).
[15] M. Jeon, Y. Tanaka, T. Shimizu, S. Shingubara. Energy Procedia **10**, 255 (2011).
[16] S. M. Pawar, B. S. Pawar, A. V. Moholkar, Electrochim. Acta **55**, 4057 (2010).
[17] T. Tanaka, D. Kawasaki, M. Nishio, Q. Guo, H. Ogawa. Phys. Status Solidi C **3**, 2844 (2006).
[18] S. M. Pawar, A. V. Moholkar, I. K. Kim, Current Appl. Phys. **10**, 565 (2010).
[19] L. Sun, J. He, H. Kong, F. Y. Yue, P. X. Yang, J. H. Chu. Sol. Energy Mater.: Sol. Cells **95**, 2907 (2011).
[20] I. Repins, C. Beall, N. Vora. Sol. Energy Mater.: Sol. Cells **101**, 154 (2012).

[21] E. R. Shaaban, I. Kansal, S. Mohamed, Ferreira, Physica B: Condensed Matter **404**, 3571 (2009).
[22] E. R. Shaaban, J. Alloys Compd. **563**, 274 (2013).
[23] J. Zhang, L. Feng, W. Cai, J. Zheng, Y. Cai, B. Li, L. Wu, Y. Shao, Thin Solid Films **414**. 113 (2002).
[24] P. A. Fernandes, P. M. P. Salomé, A. F. da Cunha, Thin Solid Films **517**, 2519 (2009).
[25] A. J. Cheng, M. Manno, A. Khare, C. Leighton, J. Vac. Sci. Technol. A **29**, 051203 (2011).
[26] E. R. Shaaban, M. El-Hagary, E. S. Moustafa, H. S. Hassan, Y. A. M. Ismail, M. Emam-Ismail, A. S. Ali, Applied Physics A: Materials Science and Processing **122**, 1 (2016).
[27] E. Yousef, A. El-Adawy, N. El Koshkhany, E. R. Shaaban, Journal of Physics and Chemistry of Solids **67**, 1649 (2006).
[28] E. R. Shaaban, A. Almohammedi, E. S. Yousef, G. A. M. Ali, K. F. Chong, A. Adel, A. Ashour, Optik **164**, 527 (2018).